


# Prognostic role of pulmonary impedance estimation to predict right ventricular dysfunction in pulmonary hypertension

Sara Louise Hungerford<sup>1,2,3,4\*</sup> , Katherine Kearney<sup>1,2,3</sup>, Ning Song<sup>1,2,3</sup>, Nicole Bart<sup>1,2,3</sup>, Eugene Kotlyar<sup>1</sup>, Edmund Lau<sup>5</sup>, Andrew Jabbour<sup>1,2,3</sup>, Christopher Simon Hayward<sup>1,2,3</sup>, David William Marshall Muller<sup>1,2,3</sup> and Audrey Adjji<sup>1,2,3,6</sup>

<sup>1</sup>Department of Cardiology, St Vincent's Hospital, Darlinghurst, Australia; <sup>2</sup>The University of New South Wales, Sydney, Australia; <sup>3</sup>Victor Chang Cardiac Research Institute, Sydney, Australia; <sup>4</sup>Department of Cardiology, Royal North Shore Hospital, Sydney, Australia; <sup>5</sup>Department of Respiratory Medicine, Royal Prince Alfred Hospital, Sydney, Australia; and <sup>6</sup>BPVF department, Macquarie University Medical School, Sydney, Australia

## Abstract

**Background** The effect of pulmonary hypertension (PH) on right ventricular (RV) afterload is commonly defined by elevation of pulmonary artery (PA) pressure or pulmonary vascular resistance (PVR). In humans however, one-third to half of the hydraulic power in the PA is contained in pulsatile components of flow. Pulmonary impedance (Zc) expresses opposition of the PA to pulsatile blood flow. We evaluate pulmonary Zc relationships according to PH classification using a cardiac magnetic resonance (CMR)/right heart catheterization (RHC) method.

**Methods** Prospective study of 70 clinically indicated patients referred for same-day CMR and RHC [60 ± 16 years; 77% females, 16 mPAP <25 mmHg (PVR <240 dynes.s.cm<sup>-5</sup>/mPCWP <15 mmHg), 24 pre-capillary (PrecPH), 15 isolated post-capillary (IpcPH), 15 combined pre-capillary/post-capillary (CpcPH)]. CMR provided assessment of PA flow, and RHC, central PA pressure. Pulmonary Zc was expressed as the relationship of PA pressure to flow in the frequency domain (dynes.s.cm<sup>-5</sup>).

**Results** Baseline demographic characteristics were well matched. There was a significant difference in mPAP ( $P < 0.001$ ), PVR ( $P = 0.001$ ), and pulmonary Zc between mPAP <25 mmHg patients and those with PH (mPAP <25 mmHg: 47 ± 19 dynes.s.cm<sup>-5</sup>; PrecPH 86 ± 20 dynes.s.cm<sup>-5</sup>; IpcPH 66 ± 30 dynes.s.cm<sup>-5</sup>; CpcPH 86 ± 39 dynes.s.cm<sup>-5</sup>;  $P = 0.05$ ). For all patients with PH, elevated mPAP was found to be associated with raised PVR ( $P < 0.001$ ) but not with pulmonary Zc ( $P = 0.87$ ), except for those with PrecPH ( $P < 0.001$ ). Elevated pulmonary Zc was associated with reduced RVSWI, RVEF, and CO (all  $P < 0.05$ ), whereas PVR and mPAP were not.

**Conclusions** Raised pulmonary Zc was independent of elevated mPAP in patients with PH and more strongly predictive of maladaptive RV remodelling than PVR and mPAP. Use of this straightforward method to determine pulmonary Zc may help to better characterize pulsatile components of RV afterload in patients with PH than mPAP or PVR alone.

**Keywords** Cardiac magnetic resonance imaging; Pulmonary arterial impedance; Right heart catheterization; Right ventricular–pulmonary arterial coupling

Received: 7 July 2022; Revised: 30 August 2022; Accepted: 15 September 2022

\*Correspondence to: Sara Hungerford, Cardiology Department, St Vincent's Hospital, Victoria St, Darlinghurst 2010, Australia. Email: [sara.hungerford@svha.org.au](mailto:sara.hungerford@svha.org.au)  
Sara Louise Hungerford and Katherine Kearney are joint first authors.

## Introduction

Owing to rapid advances in therapeutics and device technologies, it is of increasing physiological and clinical importance

to understand and predict how the right ventricle (RV) may be affected by pulmonary hypertension (PH). To study such effects, it is necessary to describe the pulmonary circulation in complete quantitative terms—including both steady-state

and pulsatile components. The effect of PH on RV afterload is commonly defined by steady-state indices. That is, an elevation of the mean pulmonary artery (PA) pressure or pulmonary vascular resistance (PVR).<sup>1</sup> Pulmonary vascular resistance, expressed as the ratio of mean pressure to mean flow in the PA, assumes that the pulmonary vasculature is a non-elastic conduit with static, non-pulsatile pressure–volume relationships.<sup>2,3</sup> In humans however, the PA is highly distensible with pulsatile energy losses 2.5 times greater than that of the systemic circulation.<sup>4,5</sup> One-third to half of the hydraulic power in the PA is contained in pulsatile components of flow, expressed as the pulmonary impedance (Z).

Characteristic pulmonary impedance (Zc) is a frequency (Hz)-dependent function encompassing information about resistive, capacitive, and inertial components of vascular hydraulic load, as well as the extent of pulse wave reflection.<sup>6</sup> Pulmonary Zc was first described in invasive studies of healthy individuals during the 1960s<sup>2,4</sup> and, simply put, represents the relationship of pulsatile pressure to flow.<sup>7</sup> Pulmonary impedance (Z) at 0 Hz is the ratio of mean PA pressure (mPAP) to mean flow (commonly known as the total peripheral resistance) and is influenced predominantly by small resistance vessels and left atrial pressure. As the frequency increases, pulmonary Z is affected by more proximal elements of the arterial tree. At higher frequencies, the PA pressure–flow ratio is decreased and oscillates around a constant value from which the characteristic impedance (Zc) is derived. Pulmonary Zc is unique in that it incorporates both steady-state and pulsatile components of hydraulic load both from the distal vasculature and proximal vessel respectively.<sup>8</sup>

It has previously been shown that PA stiffness increases early during PH, well before overt elevation of PA pressure occurs.<sup>9</sup> Yet, owing to complexities of PA flow measurement by high-fidelity pressure–flow catheters,<sup>2,4</sup> pulmonary Zc measurement is seldom performed in routine clinical practice. Cardiac magnetic resonance (CMR) remains the gold standard for RV function and volume assessment. There have also been significant advances in the non-invasive measurement of systemic Zc in healthy individuals<sup>10</sup> and cardiovascular disease states<sup>11,12</sup> using a simultaneous CMR and applanation tonometric pressure technique. The latter approach has not easily been translated to the pulmonary circulation as no reliable non-invasive method to measure PA pressure currently exists. More recently, Fukumitsu *et al.* validated a combined CMR/right heart catheterization (RHC) method to determine PVR, compliance, pulmonary Zc, and wave separation analysis in a small group of patients with chronic thromboembolic PH (CTEPH).

There is an urgent and presently unmet need to better predict the response of the RV to adapt to changes in haemodynamic loading conditions—whether it be due to pulmonary vasodilator therapies or transcatheter interventions of the tricuspid valve. Routine, accessible pulmonary Zc estimation methods remain the key to unlocking this conundrum. The

primary aims of this study were to (i) evaluate pulmonary Zc according to the PH haemodynamic classification for the first time and (ii) to determine any correlation between mPAP, PVR, pulmonary Zc, and RV indices. Our hypotheses were twofold<sup>1</sup>: that pulmonary Zc estimation would be independent of mPAP in patients with CpcPH and lpcPH, but not in those with PrecPH, and<sup>2</sup> that pulmonary Zc would be a stronger predictor of RV volumes and function than steady-state indices (mPAP and PVR).

## Methods

### Study population

All new patients referred for RHC with a clinical indication for CMR over a 12-month period were screened for participation in this study, from which 70 patients were enrolled. Indications for RHC included known or suspected PH, pre-transplantation assessment, evaluation of cardiac physiology in patients with structural heart disease, and/or heart failure assessment. The most common reasons for exclusion included unable to complete both RHC and CMR protocol, concurrent pulmonary vasodilator or inotrope therapy, significant intra-cardiac shunt ( $Q_p:Q_s > 1.5$ ) or significant (>2+) valvular pathology including tricuspid regurgitation. Inadequate RHC pressure data due to signal noise or inadequate CMR flow velocity data due to motion artefact occurred on 9% of occasions (13/140). Each patient underwent same-day RHC, followed directly thereafter by CMR.

Pre-capillary PH (PrecPH) was defined as an mPAP >20 mmHg and a PVR >240 dynes.s.cm<sup>-5</sup>. Isolated post-capillary PH (lpcPH) was defined as an mPAP >20 mmHg with a PVR <240 dynes.s.cm<sup>-5</sup> and mPCWP >15 mmHg. Combined pre- and post-capillary PH (CpcPH) was defined as an mPAP >20 mmHg and PVR >240 dynes.s.cm<sup>-5</sup> and mPCWP >15 mmHg.<sup>13</sup> The remaining patients not fitting into the haemodynamic classification were assigned to mPAP <25 mmHg group. The local hospital Human Research Ethics committee approved the study. Research was performed in accordance with local hospital guidelines and the Declaration of Helsinki. Informed consent was obtained from all participants.

### RHC

RHC was performed whilst subjects were fully awake in the supine position using a standard 7.5-Fr triple lumen Swan–Ganz catheter (Edwards Lifesciences, Irvine, CA) via the right internal jugular vein. RHC-derived measurements included right atrial pressure (RAP), systolic pulmonary artery pressure (sPAP), diastolic PAP (dPAP), mean PAP (mPAP), pulmonary artery wedge pressure (PAWP), cardiac output

(CO), and cardiac index (CI). Pulmonary vascular resistance (PVR) (expressed as  $\text{dynes.s.cm}^{-5}$ ) was calculated as:  $PVR = mPAP \text{ (mmHg)} - PCWP \text{ (mmHg)} \div CO \text{ (L/min)} \times 80$ , where *mPAP* represents mean pulmonary arterial pressure, *PCWP* represents post capillary artery wedge pressure, and *CO* represents cardiac output. Cardiac output was measured using thermodilution as the average of three measurements with <10% difference.

The PA pressure waveform was obtained in the main PA 0.5 to 1 cm distal to the pulmonic valve. These waveforms were acquired using S5 Collect software and stored with a sampling frequency of 300 Hz. Consecutive signals of PA pressure during 15–20 s without large variation were selected. To remove random noise, pressure signals were smoothed by a moving-average method for a series of 30 samples. Pressure signals were divided into each beat according to the R wave of ECG, if available, or the maximum value of the first derivative of PA or RV pressure, followed by ensemble average by 10–15 pressure beats as described previously.<sup>14</sup>

### CMR imaging acquisition

CMR studies were performed in a 3-T magnet with dedicated phased-array cardiac coil during successive end-expiratory breath-holds (Siemens Magnetom, Erlangen, Germany). Right ventricular (RV) volume and mass were obtained by contouring endocardial and epicardial borders on the short axis at end-diastolic and end-systolic phases. Short-axis images from the base to the apex of the RV were obtained with a typical slice thickness and an interslice gap of 5 mm. RV end-diastolic volume index (EDVI), RV end-systolic volume index (ESVI), and RV mass index were calculated as RV end-diastolic volume (RVEDV), RV end-systolic volume (RVESV), and RV mass divided by body surface area, respectively. Right ventricular ejection fraction (EF) was calculated as  $(RVEDV - RVESV)/RVEDV \times 100$ .<sup>15,16</sup> Volumetric flow in the main PA was measured using phase-contrast velocity quantification. Images of the main PA cross section were obtained with velocity encoding perpendicular to the imaging plane. Contours were drawn around the main PA cross-section semi-automatically. The average velocity of the main PA within the contour of each image was multiplied with the area of the contour. A volumetric flow curve was plotted with a sampling period of 12–45 ms. Both flow and the cine images were retrospectively gated by the ECG, thus ensuring that the complete cardiac cycle was covered.<sup>17</sup> All CMR analyses were performed using cvi42 (Circle Cardiovascular Imaging, Calgary, Canada).

### Haemodynamic data analysis

Pulmonary Zc (expressed as  $\text{dynes.s.cm}^{-5}$ ) was calculated using frequency domain analysis of the PA pressure and flow

velocity waveforms<sup>10,11</sup> using Matlab v18 software (Natick, MA). Flow velocity and pressure waveforms were decomposed into their component harmonics using a fast Fourier transformation (FFT) for frequencies up to 10 Hz. Any harmonics were excluded if the modulus was less than 0.1 mmHg for pressure, or less than 5 mL/s for flow velocity.<sup>18</sup> To take into account the difference in heart rate (HR) between pressure and flow measurements, harmonics were normalized and interpolated linearly into the nearest integer frequencies, that is, 1, 2, 3 ..., 10 Hz. Pulmonary Zc was estimated as the mean magnitude of impedance modulus between 2 and 10 Hz. Systemic Zc was calculated using a previously reported method of simultaneous CMR/AT acquisition.

### Statistical analysis

Data analysis was performed with SPSS-27 (IBM Corporation, Armonk, NY). Normally distributed variables are presented as means  $\pm$  SD; non-normally distributed variables are presented as median [interquartile range (IQR)], unless otherwise specified. Normality was tested by assessing the mean, median and standard deviation, and a quantile–quantile plot. Student's *t*-test or Mann–Whitney *U* test was used to compare variables between patients where appropriate. A Chi-square test was used to analyse dichotomous variables. A Pearson's correlation coefficient calculation was performed to identify any correlation with *mPAP*, *PVR*, pulmonary Zc, and other variables. *P* values < 0.05 were considered statistically significant.

## Results

The mean age of the study population was  $60 \pm 16$  years, 77% females. Fifty-four (77%) patients had evidence of PH on RHC, whereas 16 patients were assigned to the *mPAP* < 25 mmHg group. Twenty-four (34%) patients had PrecPH, 15 (21%) lpcPH, and 15 (21%) CpcPH. There were no significant differences age, sex, height, weight, or body surface area (BSA) between the *mPAP* < 25 mmHg and PH groups (all *P* > 0.05). Baseline characteristics are reported in *Table 1*.

### RHC

Resting RHC data are summarized in *Table 2*. Mean PA pressure was lowest in *mPAP* < 25 mmHg patients and highest in patients with PrecPH (*mPAP* < 25 mmHg:  $20 \pm 4$  mmHg; PrecPH:  $45 \pm 14$  mmHg; *P* < 0.001). Pulmonary vascular resistance was lowest in *mPAP* < 25 mmHg patients and highest in patients with PrecPH (*mPAP* < 25 mmHg:  $127 \pm 43$   $\text{dynes.s.cm}^{-5}$ ; PrecPH:  $492 \pm 194$   $\text{dynes.s.cm}^{-5}$ ; *P* = 0.001). There was no significant difference in SVR between *mPAP*

**Table 1** Baseline demographic characteristics

	mPAP <25 mmHg (n = 16)	PrecPH (n = 24)	lpcPH (n = 15)	CpcPH (n = 15)	P value
<b>Characteristics</b>					
Age, mean years ± SD	54 ± 17	53 ± 18	60 ± 18	64 ± 14	0.54
Sex					
Female, n (%)	13/16	17/24	12/15	12/15	N/S
Height (cm)	163 ± 9	166 ± 9	166 ± 9	168 ± 8	0.39
Weight (kg)	78 ± 18	70 ± 15	82 ± 9	82 ± 19	0.16
Body mass index	29.6 ± 6.9	25.5 ± 5.4	29.8 ± 6.2	29.1 ± 7.8	0.16
Body surface area	1.9 ± 0.2	1.8 ± 0.2	1.9 ± 0.3	2.0 ± 0.2	0.15
Atrial fibrillation	0 (0%)	6 (25%)	4 (27%)	5 (33%)	0.18
<b>Haemodynamics</b>					
Heart rate (bpm)	75 ± 11	75 ± 11	71 ± 16	76 ± 22	0.52
Brachial SBP (mmHg)	128 ± 16	124 ± 23	135 ± 23	123 ± 25	0.74
Brachial DBP (mmHg)	74 ± 10	70 ± 11	73 ± 7	73 ± 14	0.39
Mean PAP (mmHg)	20 ± 4	45 ± 14	30 ± 9	43 ± 8	<i>P</i> < 0.01
Diastolic PAP (mmHg)	14 ± 4	30 ± 17	24 ± 6	30 ± 8	<i>P</i> < 0.01
CO (L/min)	5.8 ± 1.4	4.4 ± 1.0	5.2 ± 2.1	5.5 ± 1.7	<i>P</i> < 0.01
<b>Cardiac MRI</b>					
Heart rate (bpm)	75 ± 11	73 ± 14	72 ± 19	64 ± 14	0.49
LVEF (%)	55 ± 12	63 ± 7	56 ± 22	50 ± 20	0.02
PA CSA	7.0 ± 1.9	9.9 ± 3.5	6.0 ± 1.4	9.1 ± 2.3	0.03
RVEDV (mL/m <sup>2</sup> )	154 ± 51	174 ± 59	148 ± 45	216 ± 86	1.0
RVESV (mL/m <sup>2</sup> )	77 ± 29	105 ± 50	84 ± 51	148 ± 85	0.21
RVEF (%)	50 ± 11	42 ± 12	46 ± 20	37 ± 20	0.07
RV SV (mL)	77 ± 28	68 ± 19	64 ± 31	69 ± 23	0.17
Max PA flow	339 ± 63	332 ± 136	324 ± 91	291 ± 113	<i>P</i> > 0.05
Average systolic PA flow	196 ± 41	212 ± 78	186 ± 53	186 ± 57	<i>P</i> > 0.05

bpm, beats per minute; CO, cardiac output; CpcPH, combined pre-capillary and post-capillary PH; DBP, diastolic blood pressure; EDVI, end-diastolic volume indexed; ESVI, end-systolic volume indexed; lpcPH, isolated post-capillary PH; PA, pulmonary artery; PrecPH, pre-capillary PH; RV, right ventricular; SBP, systolic blood pressure; SD, standard deviation.

**Table 2** Steady-state and pulsatile load stratified by PH classification

	mPAP <25 mmHg	PrecPH	lpcPH	CpcPH	mPAP <25 mmHg vs. all PH
mPAP (mmHg)	20 ± 4	45 ± 14	30 ± 9	43 ± 8	<i>P</i> < 0.001
SVR (dyne.s.cm <sup>-5</sup> )	1238 ± 341	1203 ± 386	1439 ± 631	1412 ± 409	0.65
PVR (dyne.s.cm <sup>-5</sup> )	127 ± 43	492 ± 194	159 ± 72	380 ± 78	0.001
Systemic Zc (dyne.s.cm <sup>-5</sup> )	84 ± 42	74 ± 29	69 ± 16	88 ± 28	0.779
Pulmonary Zc (dyne.s.cm <sup>-5</sup> )	47 ± 19	86 ± 20	66 ± 30	86 ± 39	0.05

CpcPH, combined pre-capillary and post-capillary PH; DBP, diastolic blood pressure; EDVI, end-diastolic volume indexed; ESVI, end-systolic volume indexed; lpcPH, isolated post-capillary PH; mPAP, mean pulmonary artery pressure; PH, PrecPH, pre-capillary PH; pulmonary hypertension; PVR, pulmonary vascular resistance; SBP, systolic blood pressure; SD, standard deviation; SVR, systemic vascular resistance; Zc, characteristic impedance.

<25 mmHg patients and those with PH (mPAP <25 mmHg: 1238 ± 341 dynes.s.cm<sup>-5</sup> vs. all PH: 1422 ± 618 dynes.s.cm<sup>-5</sup>; *P* = 0.65).

## CMR imaging

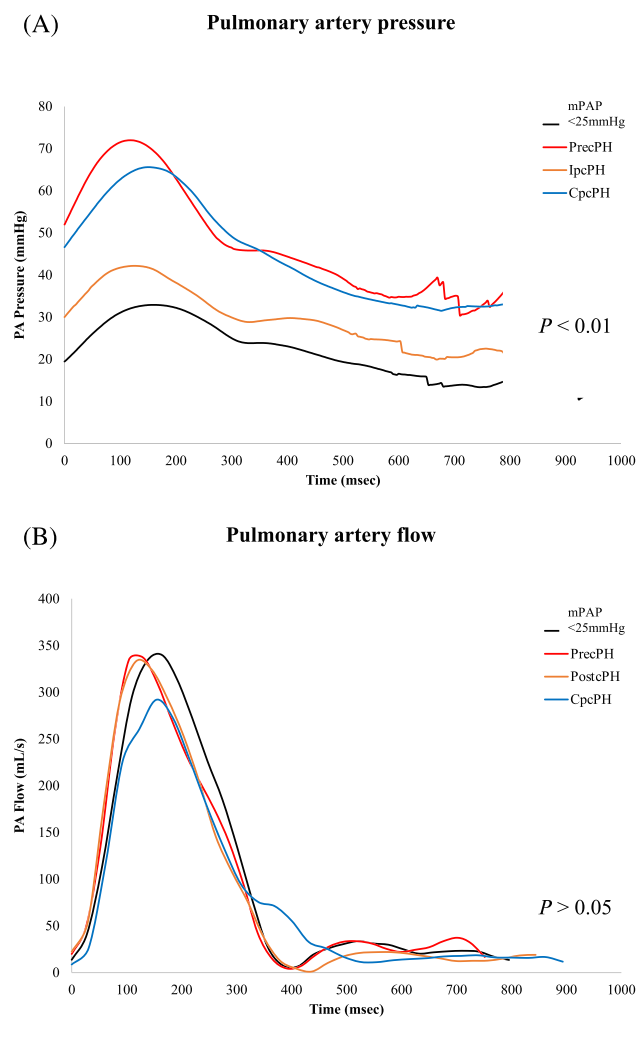
Right ventricular function and flow data are summarized in *Table 1*. Combined pre-capillary and post-capillary PH and PrecPH groups exhibited poorer RV contractility compared with the mPAP <25 mmHg and lpcPH groups as expected (RVEF mPAP <25 mmHg: 50 ± 11%; PrecPH: 42 ± 12%; CpcPH 37 ± 20%; lpcPH 46 ± 20%; *P* = 0.07). Patients with CpcPH had a trend towards larger RV end-diastolic/end-systolic volumes and increased RV stroke volume, albeit this did not reach statistical significance (all *P* > 0.05). No significant difference in

maximum or average systolic PA flow was observed between mPAP <25 mmHg patients and those with PrecPH and lpcPH (maximum systolic PA flow mPAP <25 mmHg: 339 ± 63 mL/s; PrecPH: 332 ± 136 mL/s; lpcPH 324 ± 91 mL/s; all *P* > 0.05); however, there was a trend towards reduced maximum flow in patients with CpcPH as we might have expected (CpcPH 291 ± 113 mL/s; *P* = 0.07). Pulmonary artery cross-sectional area (CSA) was significantly larger in PrecPH and CpcPH patients (*P* = 0.03). *Figure 1* shows ensemble average PA flow velocity curves from the different study populations.

## Haemodynamic data analysis

CMR was performed on the same day directly after RHC to minimize any significant alteration in haemodynamic state.

**Figure 1** (A) Ensemble average RHC-derived PA pressure waveforms from the different PH study populations. (B) Ensemble average CMR-derived flow velocity waveforms from the different PH study populations. mPAP <25 mmHg patients are represented in black. CMR, cardiac magnetic resonance imaging; PA, pulmonary artery; PH, pulmonary hypertension; RHC, right heart catheter.



Study patients had no medications or interventions between RHC and CMR and HR remained steady ( $P = N/S$ ). Pressure–flow analysis permitted quantification of pulmonary Zc and systemic Zc data, which are summarized in *Table 2*. Pulmonary Zc was significantly lower in mPAP <25 mmHg patients than in those with PH ( $P = 0.05$ ). Pulmonary Zc was highest in patients with PrecPH ( $86 \pm 20$  dynes.s.cm<sup>-5</sup>) and CpcPH ( $86 \pm 39$  dynes.s.cm<sup>-5</sup>) lowest in those with IpcPH ( $66 \pm 30$  dynes.s.cm<sup>-5</sup>;  $P < 0.05$ ). There was no significant difference in systemic Zc between mPAP <25 mmHg patients and those with PH (all  $P > 0.05$ ). *Figure 2* shows ensemble average pulmonary Zc spectra graphed as its amplitude and phase from the different study populations.

## Correlation between pulmonary Zc and other variables

A Pearson’s correlation coefficient was performed to assess correlation between mPAP, PVR, pulmonary Zc, and variables thought to be related to increased pulmonary Zc (*Table 3* and *Figure 3*). For the entire PH cohort, increased mPAP was found to be associated with raised PVR ( $P < 0.001$ ;  $R^2 = 0.78$ ) but not pulmonary Zc ( $P = 0.87$ ;  $R^2 = -0.03$ ). These findings were not uniformly observed across the different PH sub-populations however. In patients with PrecPH, increased mPAP was found to be associated with raised PVR ( $P < 0.001$ ;  $R^2 = 0.94$ ) and with pulmonary Zc ( $P < 0.001$ ;  $R^2 = 0.78$ ). However, there was no association between elevated mPAP and pulmonary Zc in patients with IpcPH and CpcPH, despite a significant correlation with PVR (IpcPH  $P = 0.03$ ,  $R^2 = 0.55$ ; CpcPH  $P = 0.01$ ,  $R^2 = 0.77$ ). Detailed Pearson’s correlation data are listed in *Table 3* and shown in *Figure 3*.

Further correlation between pulmonary mPAP, PVR, pulmonary Zc, and variables thought to be related to RV function and volumes were performed. For the entire cohort, elevated pulmonary Zc was found to be significantly associated with impaired RVSWI ( $P < 0.001$ ;  $R^2 = 0.44$ ), RVEF, and CO ( $P = 0.05$ ,  $R^2 = 0.21$ ) as well as non-significantly associated with increased RVEDV and RVESV ( $P = 0.08$ ). Weaker predictive relationships were observed between indices of steady-state load (PVR, mPAP) and RV function and volumes. Elevated PVR was associated with reduced RVSWI ( $P < 0.001$ ;  $R^2 = 0.42$ ), but not with RVEF, RVCO, or RVEDV/ESV (all  $P > 0.05$ ). There was no significant association between mPAP and RVSWI, RVEF, and RVCO (all  $P > 0.05$ ), although a correlation between raised mPAP and increased RVEDV and RVESV was observed ( $P = 0.04$ ,  $R^2 = 0.25$ ). Elevated mPAP, PVR, and pulmonary Zc were all significantly associated with increased RA volume (all  $P < 0.05$ ).

## Discussion

In this study, we demonstrate that pulmonary Zc was (i) higher in all patients with PH and (ii) that pulmonary Zc measurement was independent of elevated mean pulmonary artery pressure in patients with PH whereas PVR was not, except for those with PrecPH. Elevated pulmonary Zc was associated with reduced RVSWI, RVEF, and CO (all  $P < 0.05$ ), whereas PVR and mPAP were not. We build on previous historical invasive<sup>2,5,19</sup> and contemporary CMR feasibility studies<sup>8,14</sup> to demonstrate that only pulmonary Zc is able to provide independent information about the pulsatile pressure–flow relationships of the pulmonary vascular bed and right heart.

**Figure 2** Ensemble average pulmonary Zc spectra graphed as its (A) amplitude and (B) phase in different PH study populations (mPAP <25 mmHg patients are represented in black). Pulmonary Zc is a frequency (Hz)-dependent function encompassing information about resistive, capacitive, and inertial components of vascular hydraulic load as well as the extent of pulse wave reflection. Results are reported as spectra of amplitude and phase vs. frequency (Hz). Pulmonary Zc spectra in all patients with PH demonstrate increases of both the steady component (increased resistance) and oscillatory component (elevated pulmonary Zc as well as increased pulse wave reflection) of hydraulic load. In mPAP <25 mmHg patients (black), the first minimum occurred around 1 Hz, with little variability in the spectra, including the zero-frequency term (i.e. PVR) and pulmonary Zc. The phase remained close to zero until 2 Hz, after which it was more positive. The average pulmonary Zc was approximately 37% of the PVR. In lpcPH patients (orange), the impedance spectra resembled that of mPAP <25 mmHg patients with the first minimum occurring around 1 Hz. lpcPH patients, however, had slightly higher amplitudes of pressure for each harmonic, with the phase progressively positive after 2 Hz. The average pulmonary Zc was approximately 42% of the PVR. In PrecPH patients (red), the pulmonary Zc spectra appeared qualitatively similar to that of the systemic circulation. Amplitudes of harmonics of pressure and flow were higher, with more variability, less rounded waveforms, and steeper phase angles. The first minimum occurred around 1 Hz, and the second minimum at 5 Hz. The average pulmonary Zc was approximately 17% of the PVR. The phase remained close to zero until 2 Hz, after which it became positive. In CpcPH patients (blue), amplitudes of harmonics of pressure and flow were also higher than control and lpcPH cohorts, albeit with less variability and a pulmonary Zc to PVR ratio of 23%. CpcPH, combined pre-capillary and post-capillary PH; lpcPH, isolated post-capillary PH; PH, pulmonary hypertension; PrecPH, pre-capillary PH; PVR, pulmonary vascular resistance; Zc, characteristic impedance.

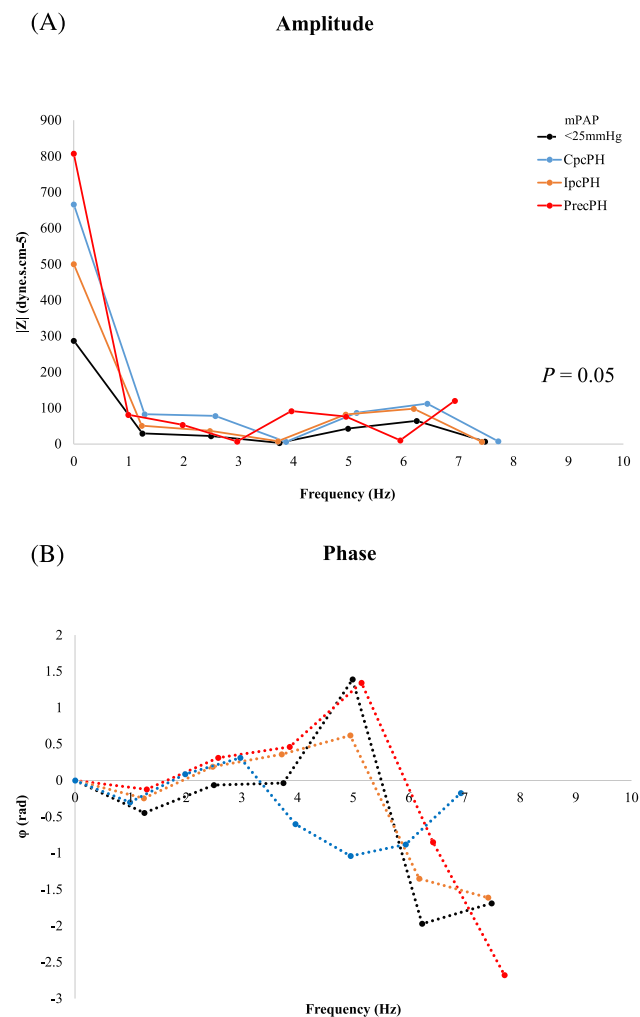
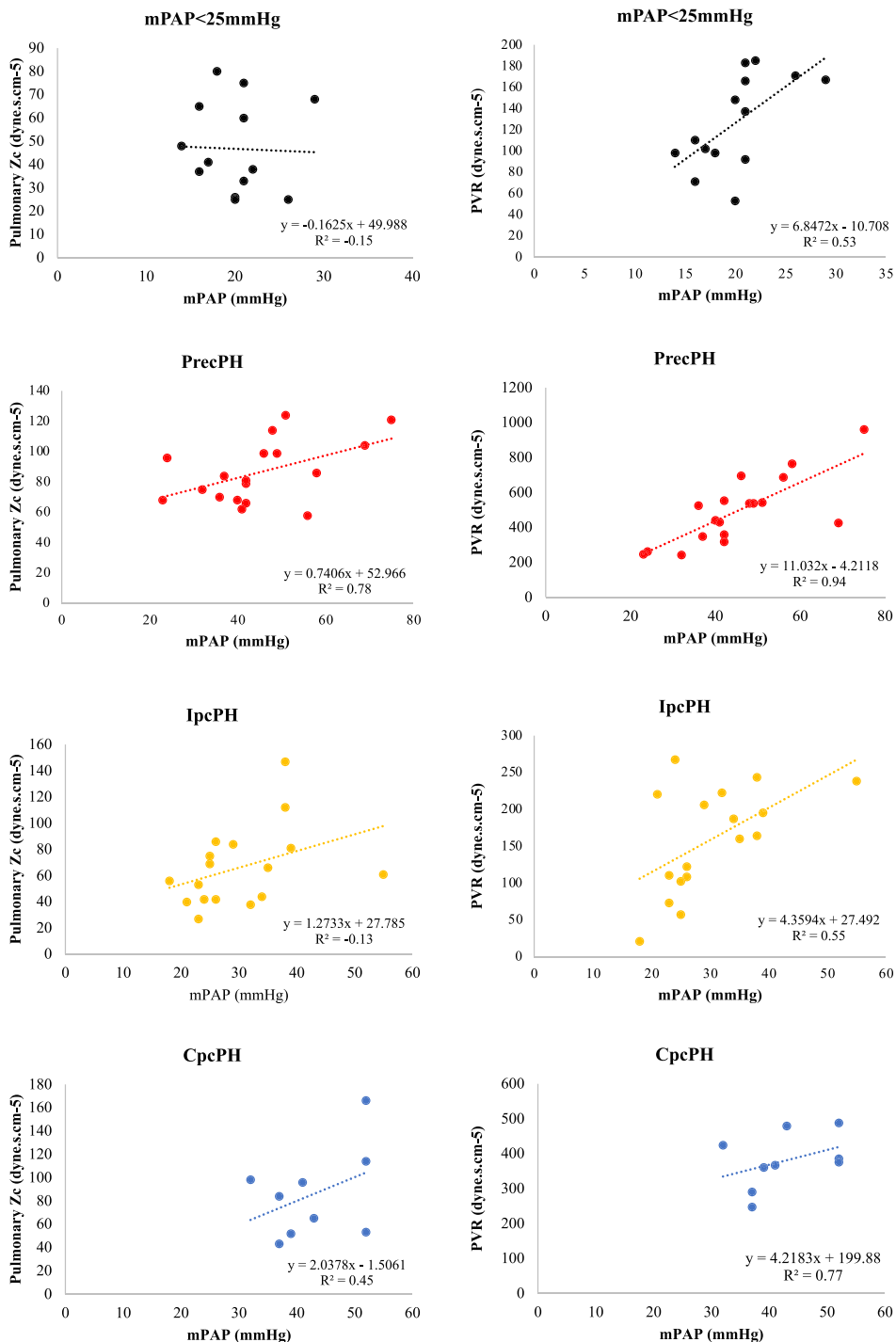


**Table 3** Pearson's correlation of PVR and Pulmonary Zc according to PH subclass

	Control	All PH	PrecPH	lpcPH	CpcPH
PVR (dyne.s.cm <sup>-5</sup> )	0.04; $R^2 = 0.53$	$P < 0.001$ ; $R^2 = 0.78$	$P < 0.001$ ; $R^2 = 0.94$	0.03; $R^2 = 0.55$	0.01; $R^2 = 0.77$
Pulmonary Zc (dyne.s.cm <sup>-5</sup> )	0.58; $R^2 = -0.15$	0.87; $R^2 = -0.03$	$P < 0.001$ ; $R^2 = 0.78$	0.64; $R^2 = -0.13$	0.17; $R^2 = 0.45$

mPAP, mean pulmonary artery pressure; PH, pulmonary hypertension; PVR, pulmonary vascular resistance; Zc, characteristic impedance.

**Figure 3** Correlation between pulmonary Zc and PVR according to PH sub-classification. There was no significant association between elevated mPAP and pulmonary Zc in patients with IpcPH and CpcPH despite correlation with PVR. CpcPH, combined pre-capillary and post-capillary PH; IpcPH, isolated post-capillary PH; mPAP, mean pulmonary artery pressure; PH, pulmonary hypertension; PrecPH, pre-capillary PH; PVR, pulmonary vascular resistance; Zc, characteristic impedance.



## Pathophysiology of haemodynamic changes in pulmonary hypertension

The most important factors influencing PA pressure are hydrostatic pressure, intra-alveolar pressure, left atrial pressure, and alveolar gases.<sup>20</sup> Increases in mean PA pressure may be passive (as a result of increased downstream pressure as in lpcPH) or hyperkinetic (as a result of increased cardiac output) or due to increased resistance from changes in the pulmonary circulation itself, as in the case of PrecPH or CpcPH to a lesser extent.<sup>20</sup> With advances in therapeutics and device technologies, it is of increasing physiological and clinical importance to understand and predict exactly how the PA is affected by PH. To study such effects, it is necessary to describe the pulmonary circulation in complete quantitative terms—including both the PVR and pulmonary Zc. Only pulmonary Zc, as demonstrated in this study, provides independent information about the pulsatile pressure–flow relationships of the pulmonary vascular bed across the spectrum of PH. That is, we found no association between elevated mPAP and pulmonary Zc in patients with lpcPH and CpcPH, despite a good correlation with PVR. There was, however, strong correlation between mPAP, PVR, and pulmonary Zc in patients with PrecPH. This finding suggests that the process of vascular wall remodelling, thrombosis, and vasoconstriction that is synonymous with PrecPH may be fixed or less reversible than other PH disease states. Monitoring pulmonary Zc response to pharmacological testing in PrecPH may yield further information about the potential treatable vasoconstrictive component of reversibility in these patients.

## Right ventricular adaptation to afterload

The normal pulmonary vascular bed is a low-pressure, low-resistance, high-compliance system capable of accommodating large increases in blood flow with minimal elevation of mPAP or PVR.<sup>21</sup> In normal physiological conditions, the right heart is coupled to the pulmonary vasculature by relative matching between contractility and afterload. As PH develops, the vascular bed becomes a high-pressure, high-resistance, low-compliance circuit that starts to resemble that of the systemic circulation.<sup>20</sup> The effect is to impart additional load on the right ventricle and alter RV-PA coupling.<sup>18</sup> Irrespective of the underlying cause, the right ventricle must adapt to the increase in afterload with compensatory hypertrophy to preserve efficient RV-PA coupling. Eventually, sustained pressure overload encumbers RV contractile performance from which RV-PA decoupling ensues.<sup>22</sup>

## Evolution of techniques to assess pulmonary impedance

Impedance of the pulmonary circulation was first described in invasive studies of healthy human subjects during cardiac

catheterisation in the 1970s and 1980s.<sup>2,4,23,24</sup> In a seminal study by Murgo *et al.*, pulmonary Zc was determined to be  $20 \pm 1$  dynes.s.cm<sup>-5</sup> (with an average mPAP ranging between 13.7 and  $14.9 \pm 0.9$  mmHg) in 10 subjects.<sup>24</sup> The pulmonary Z spectra in these subjects were qualitatively similar to the systemic Z spectra, although the ratio of PVR to Zc was smaller, with reduced phase angles due to less wave reflection. More recently, Oakland *et al.* measured pulmonary Zc and wave reflection coefficient invasively in cohort patients with varying types of PH. Oakland's pulmonary Zc values were comparable with those obtained in the present study; however, it is important to note the flow was obtained invasively using a traditional flow catheter, and Zc itself was estimated from a novel index combining RV pressure at peak flow, pressure at dP/dt (min), ejection duration, HR, and CO.

The technical aspects of custom-designed right heart multi-sensory catheters containing solid-state pressure sensors and electromagnetic flow velocity probes have been described previously.<sup>2,4,23,24</sup> Difficulties including frequency response, drift characteristics, and calibration techniques have significantly limited its widespread use.<sup>24</sup> Instead, assessment of RV afterload in clinical practice is often considered in terms of mPAP and PVR, despite one-third and one-half of the hydraulic power in the PA is contained in the pulsatile components of flow, and thus overlooked.<sup>24</sup>

Owing to complexities of invasive assessment, feasibility of transthoracic echocardiography (TTE) for pulmonary Zc measurement has been explored. In 2014, Huez *et al.* measured pulmonary Zc during RHC and Doppler echocardiography in patients with PrecPH.<sup>25</sup> Pulmonary Zc was calculated from the spectral analysis of synchronized PA pressure and flow waves in 22 patients, with a mean Zc of  $124 \pm 11$  dynes.s.cm<sup>-5</sup> and mPAP of  $63 \pm 3$  mmHg reported. Mean pulmonary Zc values were higher in this study than those by Murgo *et al.*<sup>18</sup> or observed in our cohort, owing presumably due to a higher mPAP. Nevertheless, in both the study by Huez *et al.* and in the present study, the pulmonary Zc spectra were markedly shifted to higher-than-normal pressure and flow frequencies in patients with PrecPH. Again, despite the convenience of TTE methods, RV function and flow waves obtained by Doppler echocardiography are considered less robust and reproducible than those obtained at CMR, primarily due to operator dependency and the superiority of axisymmetrical flow velocity averaging over the CSA of the PA by CMR.

In recent years, there have been significant advances in non-invasive measurement of systemic Zc in healthy human subjects<sup>10</sup> and cardiovascular disease states (i.e. obesity, hypertension, and aortic stenosis)<sup>11,12</sup> using a simultaneous CMR and AT technique (the latter from which central aortic pressure can be derived from a radial tonometer). This approach is not easily translated to the pulmonary circulation however, as no reliable non-invasive measure of PA pressure



exists. Most parameters of PA stiffness (including PA compliance, distensibility, capacitance, elasticity, and stiffness index) still require a combined approach of RHC measurement of PA pressure with non-invasive measurement of change in PA diameter or CSA within the cardiac cycle on CMR.<sup>26</sup> More recently, Fukumitsu *et al.* described the effects of chronic thromboembolic PH (CTEPH) on PA pressure waveform and RV wall stress using a combined CMR/RHC method from which the methods in this study are derived. Right heart catheter-derived PA pressure and CMR-derived PA flow data were retrospectively analysed to determine PVR, compliance, pulmonary Zc, and wave separation analysis. Fukumitsu *et al.* reported pulmonary Zc values higher than those in our study most likely due to the recruitment of CTEPH patients only. Other limitations were (i) a smaller sample size, (ii) the retrospective nature of the research, and (iii) pressure and flow curves acquired non-simultaneously (a median of 1 day apart).

To our knowledge, this is the first study to prospectively analyse PA pressure, CMR flow velocity, RV volume and function data to determine the relationship between mPAP, PVR, and pulmonary Zc according to PH haemodynamic classification. Reassuringly, we found pulmonary Zc to be most elevated in patients with PrecPH. Elevated mean PA pressure was associated with raised pulmonary Zc in patients with PrecPH, but not across the entire PH cohort or those with lpcPH and cpcPH. Our findings suggest that pulmonary Zc may be increased in patients in PH well before overt elevation of mPAP or PVR occurs. Pulmonary Z spectra were reassuringly similar to previous historical invasive studies of pulmonary Z spectra in patients both with and without PH.<sup>2,4,23,24</sup> Elevated pulmonary Zc was associated with impaired RV function and increased volumes, whereas PVR and mPAP were not uniformly.

## Limitations

We have evaluated a straightforward method by which pulmonary Zc may be estimated during routine PH workup. Our method combines 'gold standard' invasive and non-invasive tools to measure PA pressure, RV volume, and PA flow, which are then combined to provide high-quality pulmonary Zc assessment. Nonetheless, some limitations do exist. The study cohort is relatively small. We were not able to perform RHC simultaneously with CMR as performed in some other laboratories due to technical constraints. It is possible that an alteration in haemodynamic loading conditions occurred between RHC and CMR study that may have affected results to an extent; however, every care was taken to ensure stable supine resting conditions for both measurements with no significant change in HR. Given the promising preliminary results of our study, validation with a pharmacological agent to improve PA vasodilation would be beneficial.

We would expect pulmonary Zc to be more sensitive than steady-state indices to the dynamic effect of pulmonary vasodilators and inotropes. High-fidelity PA catheters may provide a higher frequency waveform for more accurate measurements but to date have significantly limited reproducibility and adoption of the technique.

## Conclusions

Assessment of RV afterload in patients with PH is often considered in terms of mPAP and PVR, and yet, this overlooks the important pulsatile contributions of hydraulic power in the PA.<sup>24</sup> We demonstrate that pulmonary Zc can be readily determined using RHC-derived pressure and CMR-derived flow data and in so doing evaluate changes to the pulmonary Zc spectrum according to PH haemodynamic classification. We demonstrate pulmonary Zc measurement to be independent of elevated mPAP in patients with PH and PVR is not, except for those with PrecPH. Elevated pulmonary Zc was more strongly associated with impaired RV contractility and increased RV volumes than steady-state indices. The ease of this technique may encourage more widespread adoption of pulmonary Zc as the importance of interaction between the pulmonary vasculature and RV function is increasingly being sought. The value of this technique in better defining patient prognosis and of predicting clinical outcomes of medical and interventional therapies for PH remains to be determined.

## Perspectives

Owing to rapid advances in therapeutics and device technologies, it is of increasing physiological and clinical importance to understand and predict how the right ventricle may be affected by PH. To study such effects, it is necessary to describe the pulmonary circulation in complete quantitative terms—including both steady-state (i.e. PVR) and pulsatile (i.e. pulmonary Zc) components. We demonstrate that pulmonary Zc can be reliably determined using a straightforward RHC/CMR method. This ease of this technique may encourage more widespread adoption of pulmonary Zc to assess RV afterload.

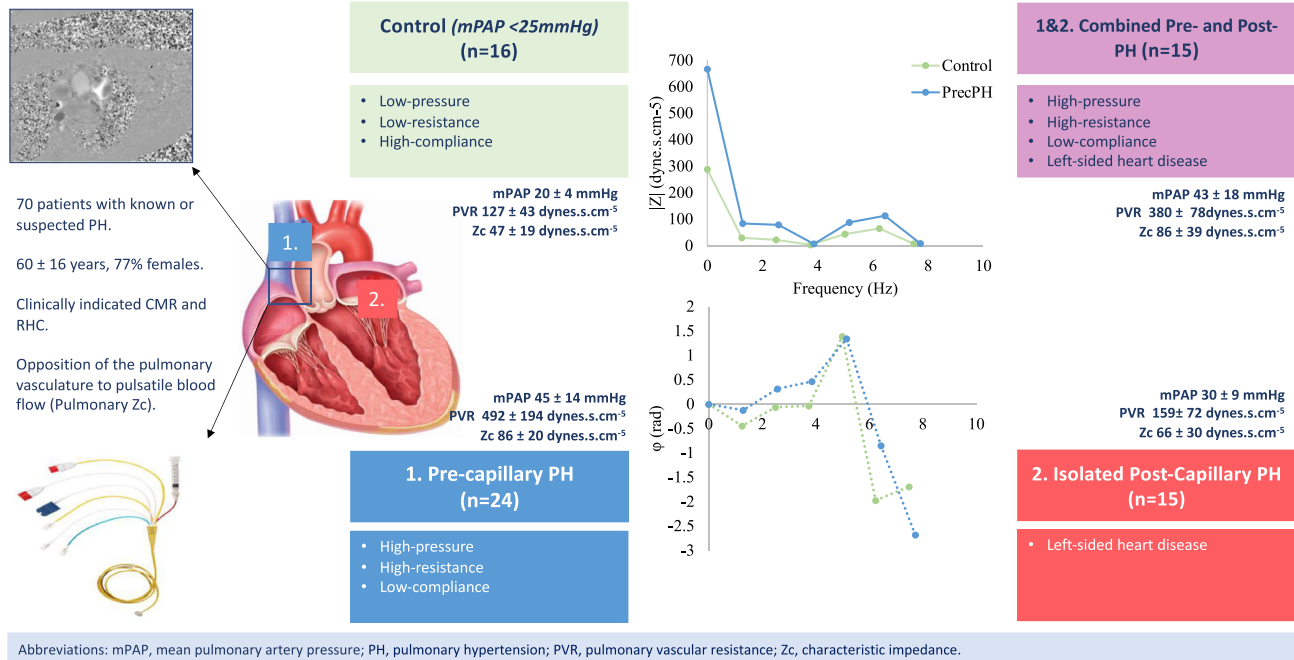
## Conflict of interest

KK is supported by an Australian Government Department of Education and Training Research Training Program grant. SLH, NS, NB, EK, EL, AJ, CSH, DWWM, and AA declare they have no conflict of interest. All authors have reported that they have no relationships relevant to the contents of this paper to disclose.

## Funding

Dr Katherine Kearney is supported by an Australian Government Department of Education and Training Research Training Program grant.

### CENTRAL ILLUSTRATION: Pulmonary characteristic impedance by cardiac magnetic resonance/right heart catheterisation.



## References

- McLaughlin VV, Archer SL, Badesch DB, Barst RJ, Farber HW, Lindner JR, Mathier MA, McGoon M, Park MH, Rosenson RS, Rubin LJ, Tapson VF, Varga J, Harrington RA, Anderson JL, Bates ER, Bridges CR, Eisenberg MJ, Ferrari VA, Grines CL, Hlatky MA, Jacobs AK, Kaul S, Lichtenberg RC, Lindner JR, Moliterno DJ, Mukherjee D, Pohost GM, Rosenson RS, Schofield RS, Shubrooks SJ, Stein JH, Tracy CM, Weitz HH, Wesley DJ, ACCF/AHA. ACCF/AHA 2009 expert consensus document on pulmonary hypertension: A report of the American College of Cardiology Foundation task force on expert consensus documents and the American Heart Association: Developed in collaboration with the American College of Chest Physicians, American Thoracic Society, Inc., and the Pulmonary Hypertension Association. *Circulation*. 2009; **119**: 2250–2294.
- Milnor WR, Conti CR, Lewis KB, O'Rourke MF. Pulmonary arterial pulse wave velocity and impedance in man. *Circ Res*. 1969; **25**: 637–649.
- Gupta A, Sharifov OF, Lloyd SG, Tallaj JA, Aban I, Dell'italia LJ, Denney TS Jr, Gupta H. Novel noninvasive assessment of pulmonary arterial stiffness using velocity transfer function. *J Am Heart Assoc*. 2018; **7**: e009459.
- Milnor WR, Bergel DH, Bargainer JD. Hydraulic power associated with pulmonary blood flow and its relation to heart rate. *Circ Res*. 1966; **19**: 467–480.
- O'Rourke MF. Vascular impedance in studies of arterial and cardiac function. *Physiol Rev*. 1982; **62**: 570–623.
- Laskey WK, Ferrari VA, Palevsky HI, Kussmaul WG. Pulmonary artery hemodynamics in primary pulmonary hypertension. *J Am Coll Cardiol*. 1993; **21**: 406–412.
- Morpurgo M, Jezek V, Ostadal B. Pulmonary input impedance or pulmonary vascular resistance? *Monaldi Arch Chest Dis*. 1995; **50**: 282–285.
- Oakland H, Joseph P, Naeije R, Elassal A, Cullinan M, Heerdt PM, Singh I. Arterial load and right ventricular-vascular coupling in pulmonary hypertension. *J Appl Physiol (1985)*. 2021; **131**: 424–433.
- Sanz J, Kariisa M, Dellegrattaglia S, Prat-González S, Garcia MJ, Fuster V, Rajagopalan S. Evaluation of pulmonary artery stiffness in pulmonary hypertension with cardiac magnetic resonance. *J Am Coll Cardiol Img*. 2009; **2**: 286–295.
- Adji A, Kachenoura N, Bollache E, Avolio AP, O'Rourke MF, Mousseaux E. Magnetic resonance and applanation tonometry for noninvasive determination of left ventricular load and ventricular vascular coupling in the time and frequency domain. *J Hypertens*. 2016; **34**: 1099–1108.
- Namasivayam M, Adji A, Lin L, Hayward CS, Feneley MP, O'Rourke MF, Muller DWM, Jabbour A. Non-invasive quantification of ventricular contractility, arterial elastic function and ventriculo-arterial coupling from a single diagnostic encounter using simultaneous arterial tonometry and magnetic resonance imaging. *Cardiovasc Eng Technol*. 2020; **11**: 283–294.

12. Hungerford SL, Adji AI, Bart NK, Lin L, Namasivayam MJ, Schnegg B, Jabbour A, O'Rourke MF, Hayward CS, Muller DWM. A novel method to assess valvulo-arterial load in patients with aortic valve stenosis. *J Hypertens*. 2020; **39**: 437–446.
13. Simonneau G, Montani D, Celermajer DS, Denton CP, Gatzoulis MA, Krowka M, Williams PG, Souza R. Haemodynamic definitions and updated clinical classification of pulmonary hypertension. *Eur Respir J*. 2019; **53**: 1801913.
14. Fukumitsu M, Westerhof BE, Ruigrok D, Braams NJ, Groeneveldt JA, Bayoumy AA, Marcus JT, Meijboom LJ, de Man FS, Westerhof N, Bogaard HJ, Vonk Noordegraaf A. Early return of reflected waves increases right ventricular wall stress in chronic thromboembolic pulmonary hypertension. *Am J Physiol Heart Circ Physiol*. 2020; **319**: H1438–h50.
15. Trip P, Rain S, Handoko ML, van der Bruggen C, Bogaard HJ, Marcus JT, Boonstra A, Westerhof N, Vonk Noordegraaf A, de Man FS. Clinical relevance of right ventricular diastolic stiffness in pulmonary hypertension. *Eur Respir J*. 2015; **45**: 1603–1612.
16. van de Veerdonk MC, Kind T, Marcus JT, Mauritz GJ, Heymans MW, Bogaard HJ, Boonstra A, Marques KMJ, Westerhof N, Vonk-Noordegraaf A. Progressive right ventricular dysfunction in patients with pulmonary arterial hypertension responding to therapy. *J Am Coll Cardiol*. 2011; **58**: 2511–2519.
17. Lankhaar JW, Westerhof N, Faes TJ, Marques KM, Marcus JT, Postmus PE, Vonk-Noordegraaf A. Quantification of right ventricular afterload in patients with and without pulmonary hypertension. *Am J Physiol Heart Circ Physiol*. 2006; **291**: H1731–H1737.
18. Kussmaul WG, Wieland JM, Laskey WK. Pressure-flow relations in the pulmonary artery during myocardial ischaemia: Implications for right ventricular function in coronary disease. *Cardiovasc Res*. 1988; **22**: 627–638.
19. Piene H. Pulmonary arterial impedance and right ventricular function. *Physiol Rev*. 1986; **66**: 606–652.
20. Chemla D, Castelain V, Hervé P, Lecarpentier Y, Brimiouille S. Haemodynamic evaluation of pulmonary hypertension. *Eur Respir J*. 2002; **20**: 1314–1331.
21. Verhoeff K, Mitchell JR. Cardiopulmonary physiology: Why the heart and lungs are inextricably linked. *Adv Physiol Educ*. 2017; **41**: 348–353.
22. Vanderpool RR, Saul M, Nouriaie M, Gladwin MT, Simon MA. Association between hemodynamic markers of pulmonary hypertension and outcomes in heart failure with preserved ejection fraction. *JAMA Cardiol*. 2018; **3**: 298–306.
23. Braunwald E, Gabe IT, Gault J, Mason DT, Mills CJ, Shillingford JP. Vascular impedance in man. *J Physiol*. 1969; **202**: 10p.
24. Murgu JP, Westerhof N. Input impedance of the pulmonary arterial system in normal man. Effects of respiration and comparison to systemic impedance. *Circ Res*. 1984; **54**: 666–673.
25. Huez S, Brimiouille S, Naeije R, Vachiéry JL. Feasibility of routine pulmonary arterial impedance measurements in pulmonary hypertension. *Chest*. 2004; **125**: 2121–2128.
26. Freed BH, Collins JD, François CJ, Barker AJ, Cuttica MJ, Chesler NC, Markl M, Shah SJ. MR and CT imaging for the evaluation of pulmonary hypertension. *J Am Coll Cardiol Img*. 2016; **9**: 715–732.